ACADEMIC PRESS

Analytical Biochemistry 307 (2002) 63–69

ANALYTICAL BIOCHEMISTRY

www.academicpress.com

Sensitivity and accuracy of quantitative real-time polymerase chain reaction using SYBR green I depends on cDNA synthesis conditions

Ronald H. Lekanne Deprez,* Arnoud C. Fijnvandraat, Jan M. Ruijter, and Antoon F.M. Moorman

Experimental and Molecular Cardiology Group, Academic Medical Center, Meibergdreef 15, 1105 AZ Amsterdam, The Netherlands

Received 25 June 2001

Abstract

The recent development of real-time PCR has offered the opportunity of sensitive and accurate quantification of mRNA levels that is crucial in biomedical research. Although reverse transcription (RT)-PCR is at present the most sensitive method available, many low abundant mRNAs are, although detectable, often not quantifiable. Here we report an improved two-step real-time RT-PCR procedure using SYBR green I and the LightCycler that better permits accurate quantification of mRNAs. Omission of dithiothreitol from the cDNA synthesis reaction was found to be crucial. This resulted in a lower cycle number at which the cDNA level is determined (C_T value), steeper amplification curves, and removal of background fluorescence in the subsequent PCR. In addition, the choice of the cDNA priming oligo can improve detection sensitivity even further. In contrast to hexamer primer usage, both gene-specific and oligo-dT_{VN} priming were very efficient and accurate, with gene-specific priming being the most sensitive. Finally, accurate quantification of mRNAs by real-time PCR using SYBR green I requires verification of the specificity of PCR by both melting curve and gel analysis.

Keywords: mRNA expression; Quantification; SYBR green I; Real-time RT-PCR; cDNA synthesis; DTT

The intensive development of technologies for quantification of nucleic acids over the past decade reflects their importance in diagnostics and biomedical research. Recently, the development of new fluorescent techniques has led to novel PCR-based assay formats that greatly simplify current protocols [1]. These formats allow real-time detection of PCR products, offering the advantage that data can be collected in the log linear phase of the PCR reaction, which is considered the condition of constant amplification efficiency [2]. Other PCR-based methods make use of end point analyses, in which decrease of reagent concentration, product inhibition, enzyme instability, and competition of reannealing amplification product with primer interfere with an accurate analysis [3]. With real-time PCR it is possible to measure the number of cycles necessary to detect a signal (threshold cycle) and use this to determine the starting level of a certain mRNA present in the mRNA preparation. In principle, two fluorescent formats for correlating the amount of PCR product with fluorescence signals are available. The first one allows specific sequence detection because of the use of fluorescently labeled sequence-specific hybridization probes. Several types of probes (TaqMan, Molecular Beacons, LightCycler, and Amplifluor) can be used, all based on fluorescence resonance energy transfer [4,5]. The second format uses the DNA binding dye, SYBR green I. This dye binds in the minor groove of double-stranded DNA in a sequence-independent way. When it binds, its fluorescence increases over 100-fold.

The aim of this investigation is to improve the sensitivity and accuracy of the two-step reverse transcrip-

* Corresponding author. Fax: +31-20-6976177.
E-mail address: r.h.lekanne@amc.uva.nl (R.H. Lekanne Deprez).

0003-2697/02/$ - see front matter
PII: S0003-2697(02)00021-0

Table 1
Primer characteristics

Gene	Species	GenBank Acc. no.	Forward primer[a]	Reverse primer[a]	Amplicon size (bp)
GATA4	Mouse	NM_008092	1684–1704	1815–1834	151
Nkx2.5	Mouse	NM_008700	1315–1334	1452–1471	157
MEF2C	Mouse	L13171	1326–1345	1455–1476	151
GAPDH	Mouse	M32599	478–497	717–698	239
ANF	Mouse	K02781	593–612	809–831	136
Elongation factor 1α	Mouse	X13661	1405–1424	1542–1560	156
HPRT	Mouse	J00423	576–593	805–824	248
PBGD	Mouse	M286643	505–521		126
	Mouse	M28664		70–89	

[a] Coordinates according to GenBank.

tion (RT)-PCR[1] reaction using SYBR green I to facilitate quantification, especially in the case of low abundant mRNAs.

Materials and method

Cell culture, RNA isolation, and DNAse I treatment

D3 embryonic stem (ES) cells were differentiated using the hanging drop assay as described by Maltsev et al. [6], resulting in cardiac differentiation. Total RNA was isolated from differentiating ES cells and adult mouse heart using an RNA isolation kit (RNeasy, Qiagen) according to the manufacturer's instructions. To remove contaminating genomic DNA, the RNA preparation (10–100 μg) was subsequently incubated with 10 units RQ1 RNase-free Dnase (Promega, M6101) for 30 min at 37 °C, extracted with phenol and chloroform, and finally precipitated and dissolved in 3 mM Tris–HCl, pH 7.5/0.2 mM EDTA. The total RNA concentration was determined spectrophotometically at 260 nm. RNA integrity was electrophoretically verified.

Primer design

Complementary DNA PCR primers for the mouse were designed using Oligo primer analysis (version 4.1, National Biosciences) and Primer Express (version 1.0, PE Applied Biosystems) software from DNA and RNA sequences obtained from GenBank (Table 1). All primer sets had a calculated annealing temperature of 58 °C (nearest neighbor method). Primers were ordered from Biolegio (The Netherlands).

Reverse transcription

First-strand complementary DNA was synthesized by priming with oligo-dT_{14VN} (Biolegio), hexamers (Roche, 1034731) or a gene-specific primer. Oligo-dT_{14VN}, containing a lock docking site (VN) at the 3′ end, was obtained by making each of the 12 hexadecamer combinations separately, which were added together in equimolar amounts. This primer has the advantage that cDNA synthesis starts at the boundary poly-A-tail and mRNA. In other experimental systems the introduction of this site improved the detection sensitivity significantly [7,8]. The reverse transcription was performed in 25-μl reactions using varying concentrations of $MgCl_2$ and dithiothreitol (DTT) and two different buffers: PCR buffer (buffer P) containing 75 mM Tris–HCl pH 9.0, 20 mM $(NH_4)_2SO_4$, and 0.01% Tween 20 and first-strand buffer (buffer F) containing 50 mM Tris–HCl, pH 8.3, and 75 mM KCl. The priming oligo (125-pmol oligo-dT_{14VN} or 125-pmol hexamer or 40-pmol gene-specific primer) was annealed to 1 μg of total RNA in a total volume of 10 μl by incubation at 70 °C for 10 min and cooling down to 4 °C (PTC 200, MJ Research). Reverse transcription was performed by the addition of 15 μl RT mix such that the final concentration was 1× buffer, 0.5 mM dNTP, 0–20 mM DTT, 1.25–5 mM $MgCl_2$ and 100 U superscript II (Gibco-BRL) and the mixture was incubated at 42 °C for 60 min, heated to 70 °C for 15 min, and cooled to 4 °C (PTC 200, MJ Research). Finally, 25 μl of a 3 mM Tris–HCl, pH 7.5/0.2 mM EDTA solution was added. When cDNA conditions were compared the same master mixes were used. To determine the presence of contaminating genomic DNA, reverse transcriptase was omitted in the cDNA synthesis reaction. A specific product was never observed (data not shown). In addition, reverse transcription in the absence of priming oligo was performed. This resulted in a specific product, which appeared at least 10 cycles later than with priming oligo and is probably the result of the non-primer cDNA synthesis background in the RNA preparation (data not shown).

Polymerase chain reaction

PCR amplification and analysis were achieved using a LightCycler instrument (Roche) and software version

[1] *Abbreviations used*: RT, reverse transcription; ES, embryonic stem; DTT, dithiothreitol.

3.0, respectively (Roche). For each primer combination optimal $MgCl_2$ (2, 3, 4, 5 mM) concentration and annealing temperature (56, 58, 60, 62, 64 °C) were experimentally determined. For all primer pairs but PBGD used in this study 4 mM $MgCl_2$ and an annealing temperature of 58 °C was most optimal. The PBGD primers performed most optimally at 2 mM $MgCl_2$. The reaction mixture consisted of cDNA (2 μl), 0.5 μM of each primer, 1.5 μl LightCycler FastStart DNA Master SYBR Green 1 mix (Roche, 2239264), and $MgCl_2$ in a total volume of 15 μl. cDNA conditions to be compared were made with the same PCR master mixes and within a single LightCycler run. All templates were amplified using the following LightCycler protocol. The fluorimeter gain for channel 1 was set to 5. The FastStart polymerase was activated and cDNA denatured by a preincubation for 10 min at 95 °C; the template was amplified for 40 cycles of denaturation for 15 s at 95 °C, annealing of primers at 58 °C programmed for 5 s, and extension at 72 °C for 10 s. Fluorescent data were acquired during each extension phase. After 40 cycles a melting curve was generated by heating the sample to 95 °C programmed for 0 s followed by cooling down to 60 °C for 15 s and slowly heating the samples at 0.1 °C/s to 95 °C while the fluorescence was measured continuously. Fast loss of fluorescence is observed at the denaturing/melting temperature of a DNA fragment, which is a unique feature of that fragment [9]. The melting peak can be obtained by plotting the negative first derivative of fluorescence against temperature. Finally, the samples were cooled down to 40 °C for 30 s. Product identity was confirmed by sequence analysis and electrophoresis on a 10% nondenaturing polyacrylamide gel stained with ethidium bromide afterward.

Standard curve

Standard curves were generated from cDNAs made from increasing amounts of total RNA (0.125, 0.25, 0.50, 1.0, 2.0, 4.0 μg). With the use of the LightCycler quantification software the threshold cycle (C_T) was determined when the noise band was set to 1 (Fig. 7a). The C_T values were subsequently used to calculate and plot a linear regression line by plotting the logarithm of template concentration (X-axis) against the corresponding threshold cycle (Y-axis). The quality of the standard curve can be judged from the slope and the correlation coefficient (r). The slope of the line can be used to determine the efficiency of target amplification ($=Ex$) using the equation $Ex = (10^{-1/\text{slope}}) - 1$, a mathematic derivative of $X_n = X_0 * (1 + Ex)^n$ with $X_n =$ number of target molecules at cycle n, $X_0 =$ initial number of target molecules, $n =$ number of cycles. In theory this slope should not be lower than −3.3 because this implies a PCR efficiency of more than 1 (>100%)

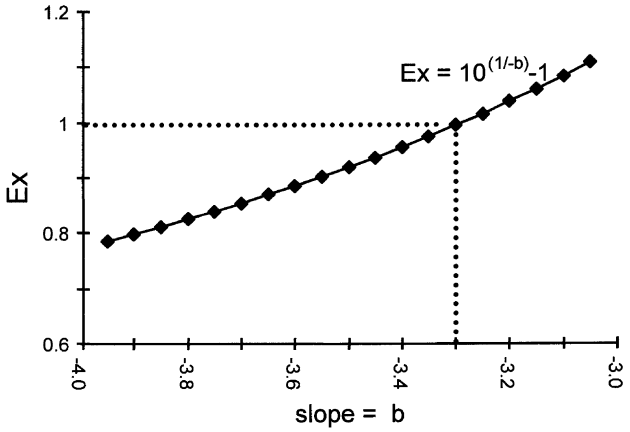

Fig. 1. Mathematic relation between efficiency of target amplification (Ex) and slope of the standard curve. 100% PCR efficiency corresponds to an Ex value of 1 (dotted line). For more details see Standard Curve under Materials and method.

and indicates that more than twice as many amplicons are being made per PCR cycle. The mathematic relation between efficiency of target amplification and slope is shown in Fig. 1. Finally, the correlation coefficient (r) shows whether a linear relation is observed: when it equals −1 this is the case.

Results and discussion

When starting real-time RT-PCR experiments we were confronted with the following problems. The quality of amplification was insufficient to allow reliable quantification and the expression of many mRNAs was too low to allow accurate quantification. In our research we are interested in the molecular cardiac phenotype of differentiated ES cells to study to what extent in vitro differentiation of ES cells represents in vivo cardiogenesis. For that purpose we started to measure the expression of several transcription factors implicated in cardiac development (e.g., Irx members [11]), other cardiac-specific genes (e.g., ANF), and generally expressed genes (GAPDH, HPRT, EF1a) by real-time RT-PCR. For all primer sets we were confronted with the following problems. The quality of amplification was insufficient to allow reliable quantification. In addition, the expression of ANF in the ES cells and the Irx transcription factors in both heart and ES cells was too low to allow accurate quantification because in these cases no product or only nonspecific product or both specific and nonspecific products was amplified at the end of PCR. In this study we set out to test whether the quality and sensitivity of the quantitative real-time RT-PCR reactions could be improved. All experiments described below were done for at least two independent RNA samples (adult mouse heart and ES-D3 cells) and several primer sets.

Confirmation of primer specificity

SYBR green I, a dye that emits light only when bound to double-stranded DNA, allows detection of DNA in a sequence-independent way. This means that when both specific and nonspecific PCR fragments are formed they will be measured. To visualize nonspecific PCR a melting curve analysis can be performed, as different fragments will usually appear as separate distinct melting peaks. The PCR reactions were checked by both melting curve and gel analysis. Generally, melting curve and gel analysis were in agreement, but in a minority of cases a single melting peak was produced, whereas on gel several bands were observed (Fig. 2) and vice versa a single band and several melting peaks (data not shown). Therefore, only primer sets that produced a single melting peak, a single prominent band of expected size on gel, and the expected nucleotide sequence were used for further analysis.

The second fluorescent detection format is based on the use of sequence-specific fluorescently labeled hybridization probes. Because only the specific PCR product is detected this method suggests high specificity and accuracy. However, unwanted products can be formed but remain undetected, which may have profound effects on the synthesis of the specific product. Both detection formats (SYBR green and hybridization probes) have about the same detection limit, reproducibility, and dynamic range (Technical Note LC 11/2000, Roche). Therefore, we prefer the use of SYBR green 1, which is, moreover, much cheaper.

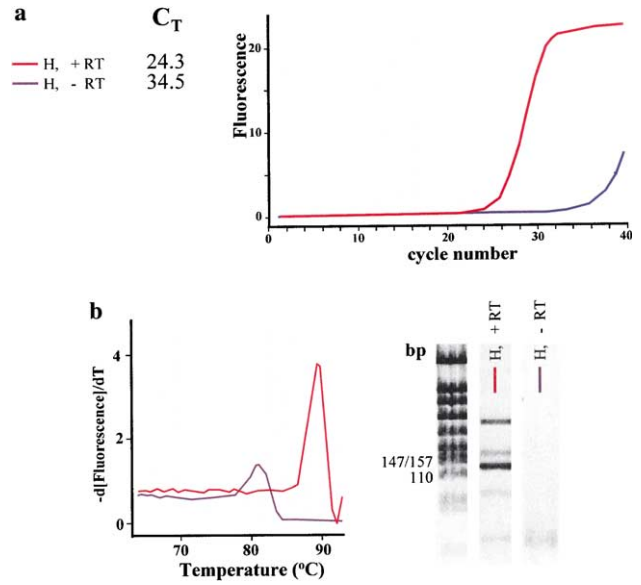

Fig. 2. Melting curve and gel analysis of the PBGD transcript. Amplification (a), melting curves (b), and gel (c) analysis for the PBGD gene using as a template cDNA made from 1 μg total adult mouse heart RNA (H) primed with oligo-dT_{VN} with (+RT) or without (−RT) reverse transcriptase. The expected amplicon size for the PBGD gene is 126 bp. A single melting peak results in several fragments on gel from which one has the expected size. Therefore, both melting curve and gel analyses are required for a reliable quantification.

Influence of buffer and $MgCl_2$ concentration on cDNA synthesis

The relative efficiency of first-strand cDNA synthesis was investigated for two RT buffers (F and P) at various $MgCl_2$ concentrations. The efficiency was measured by real-time PCR for four different primer pairs by comparing the threshold cycles (Figs. 3 and 5b). For all primer sets tested buffer F with 5 mM of $MgCl_2$ was always optimal. When the most and least optimal conditions are compared and averaged for the three-primer sets shown in Fig. 3 a difference of 2.7 ± 0.6 cycles (average $\pm$ SD) was found.

What determines the quality of amplification?

When undiluted cDNA is added to the PCR reaction high background fluorescence and shallow amplification

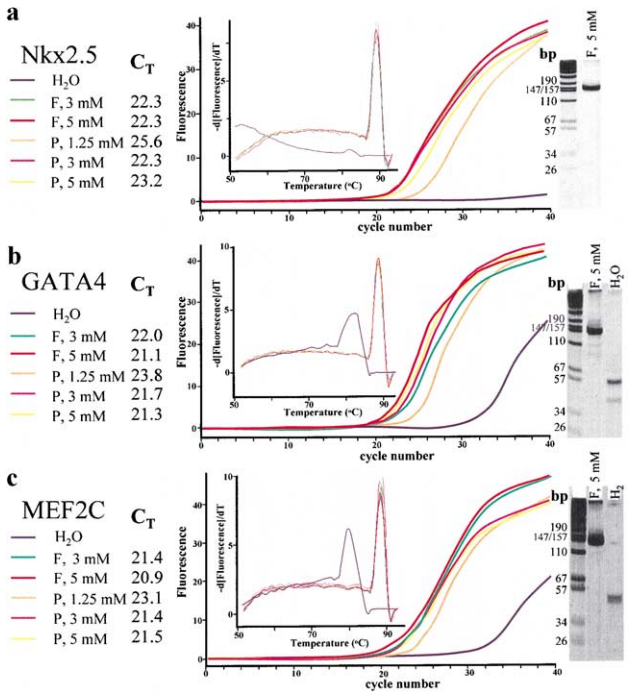

Fig. 3. Influence of buffer and $MgCl_2$ concentration on cDNA synthesis. Relative efficiency of first-strand cDNA synthesis was measured for two RT buffers (F and P) in combination with, for F, two (3, 5 mM) and, for P, three (1.25, 3, 5 mM) $MgCl_2$ concentrations by comparing the threshold cycles (C_T) after real-time PCR using SYBR green I. cDNA made from 1 μg of total RNA primed with oligo-dT_{VN} was used as a template. H_2O was used as a negative control. For each primer set Nkx2.5 (a), GATA4 (b), and MEF2C (c) C_T values, amplification curves, melting curves, and gel analysis for the different conditions are shown. Both melting curves and gel analyses show a single peak and band of the expected size. For all primer sets tested buffer F with 5 mM of $MgCl_2$ was always optimal.

curves are observed. To allow quantification it is recommended by the company to dilute the cDNA, which implies a reduction in detection sensitivity. Fig. 4 shows an example. Only lower cDNA and concomitant DTT concentrations (at least 20-fold dilution) yield curves with comparably steep slopes and the expected differences in C_T values. The confounding factor turned out to be DTT and to some extent buffer P (Figs. 5a and b). Under all conditions the proper product was made based on melting curve and gel analysis. This suggests that DTT, an agent that protects disulfide bridges from oxidation and is often added to enzyme reactions for stabilization, interferes with dye binding or fluorescence yield. In the presence of even low DTT concentrations high background fluorescence and shallow amplification curves do not permit the calculation of reliable C_T values. Therefore, to determine whether DTT interfered with the amount of cDNA produced during first-strand cDNA synthesis, cDNA synthesis reactions were performed in the presence of 0, 2, and 10 mM DTT and measured indirectly by LightCycler PCR in 20-fold diluted samples. Because this results in comparable PCR efficiencies, the C_T values of the samples can be compared (Fig. 5c). Without DTT a lower C_T value is obtained, indicating a higher level of the transcript in the cDNA preparation (Fig. 5c). Therefore, the results show that DTT is not essential and only negatively interferes with RT-PCR using SYBR green I.

An example of the effect of DTT on the quantification of a low abundant transcript is shown in Fig. 6. In differentiating ES cells ANF mRNA levels are about 575-fold lower than in adult hearts [10]. Consequently, quantification of the transcript is difficult. In the presence of DTT quantification turned out to be unreliable because of a shallow slope, high background fluorescence, and the presence of a nonspecific product (Figs. 6a–c). After sample dilution no background fluorescence

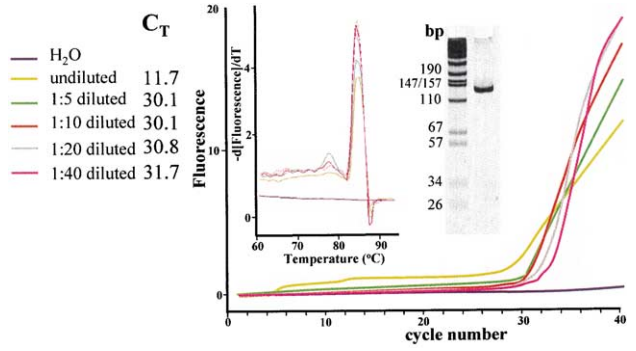

Fig. 4. Amplification quality observed by real-time RT-PCR using SYBR green I. Amplification curves, melting curves, and gel analysis for the ANF transcript with cDNA made with 10 mM DTT from ES-D3 RNA. H_2O is used as a negative control. Undiluted cDNA results in high background level of fluorescence and a very shallow amplification curve. Diluting the cDNA sample more than 20-fold results in a much steeper amplification curve without background fluorescence.

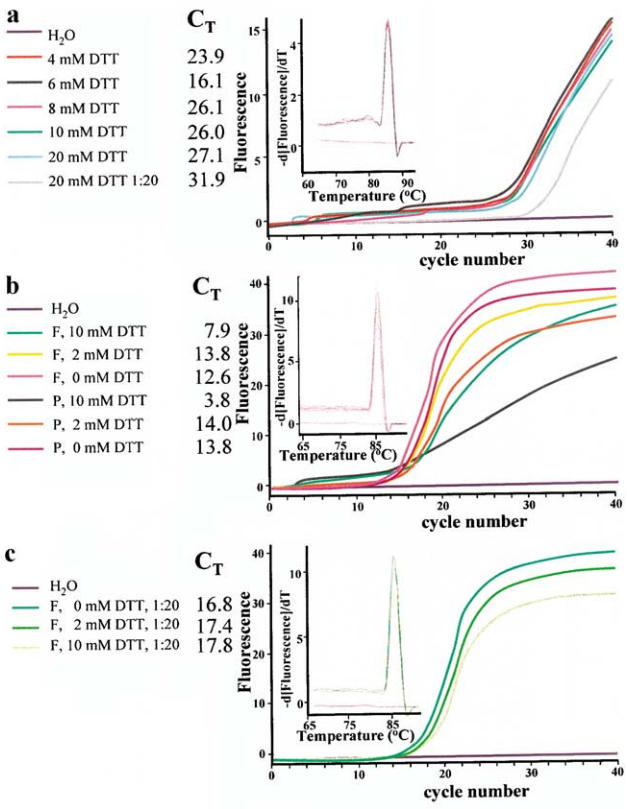

Fig. 5. Influence of RT buffer and DTT concentration on amplification quality. Amplification and melting curves for the ANF gene using cDNA made from 1 μg total RNA primed with oligo-dT_{VN} as a template. H_2O was used as a negative control, (a) cDNA was made with buffer F and increasing DTT concentrations (between 4 and 20 mM). High background fluorescence and shallow amplification curves are observed in all cases, except when one of the samples is diluted 20-fold, (b) Two RT buffers (F and P) and three DTT concentrations (0, 2, 10 mM) are compared. The degree of background fluorescence and the slope of the amplification curve were related to the concentration of DTT added to the cDNA synthesis reaction. The C_T value, at 0 mM DTT, for buffer F is 1.2 cycles lower than for buffer P. (c) Analysis of 20-fold diluted samples, which allows comparison of product yield (C_T values), suggests that cDNA synthesis without DTT is the most efficient.

and a steeper PCR curve are obtained; however, due to the nonspecific products no quantification is allowed. Without DTT PCR amplification has improved such that quantification became possible. A C_T value of 27.4 corresponds to 36 ANF molecules as determined using a standard curve generated from concentration series of PAGE gel purified PCR fragment (data not shown).

cDNA priming method and product yield

To further improve the sensitivity of the two-step real-time RT-PCR reaction several priming methods for first-strand cDNA synthesis were compared on: (1) linearity of product amplification and (2) product yield. To this end cDNA was made from increasing amounts of total RNA (Fig. 7a) using three different cDNA priming

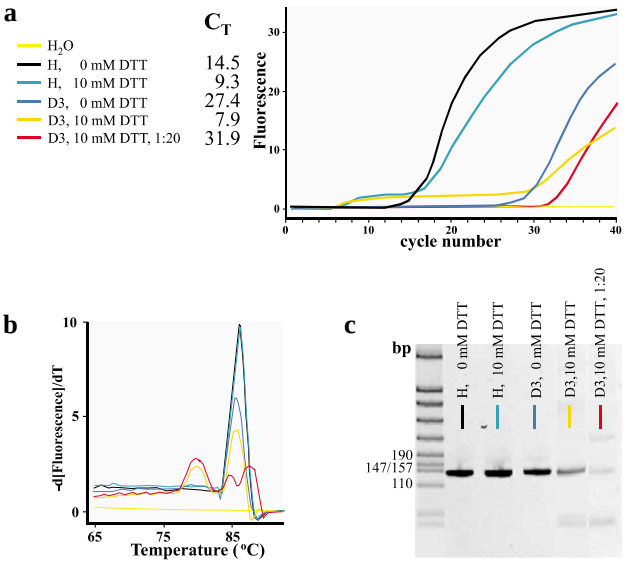

Fig. 6. Influence of DTT on quantification of a rare transcript. Amplification (a), melting curves (b), and gel analysis (c) for the ANF gene on cDNA made from 1 μg total RNA isolated from differentiating D3 cells and isolated from adult mouse heart (H) primed with oligo-dT_{VN}. H_2O was used as a negative control. cDNA was made with (10 mM) or without (0 mM) DTT. Undiluted and 20-fold dilution (1:20) cDNA have been used as a template for PCR. In contrast to D3 cDNA made in the presence of DTT, D3 cDNA without DTT resulted in a steep amplification curve and amplification of the specific product only, thereby allowing quantification.

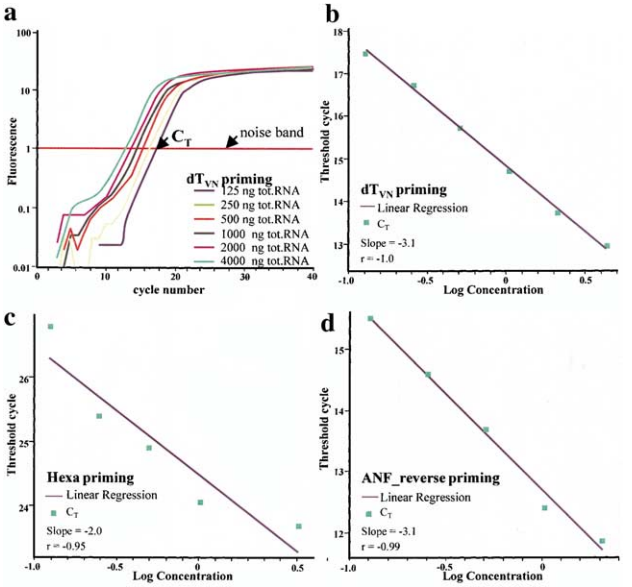

Fig. 7. Role of cDNA priming on standard curve and detection sensitivity for the ANF transcript, (a) The crossing point of the noise band with the amplification curve is the threshold cycle (C_T values). C_T values were determined with a noise band set on 1. These C_T values were used to calculate and plot the standard curves. These curves were obtained from LightCycler RT-PCR reactions with SYBR green I using cDNA made from increasing amounts of total RNA (0.125–4.0 μg) and three priming methods oligo-dT_{VN} (b), hexamer (c), and ANF reverse oligo (d).

oligos: oligo-dT_{VN} (Fig. 7b), hexamers (Fig. 7c), and gene-specific oligos (Fig. 7d). Linearity of product amplification was judged from the slope (PCR efficiency) and the correlation coefficient (r) of the standard curve. To determine which priming oligo is more efficient, product yield was determined by comparing threshold cycles after PCR. Fig. 7 shows the standard curves for the ANF transcript using three RT-priming methods. Table 2 summarizes the results for five different primer pairs. As can be seen, both oligo-dT_{VN} and gene-specific priming work efficiently, because almost all standard curves had a correlation coefficient (r) of −1 with PCR efficiencies ranging between 70 and 110%. In contrast, hexamer priming showed only good standard curves when GAPDH and MEF2C were amplified. In all other cases the correlation coefficients were poorer than −0.95 (no true linear relation), not permitting the calculation of PCR efficiencies. Indeed, erroneous efficiencies were

Table 2
Effect of cDNA priming on standard curve and detection sensitivity

PCR primers	cDNA priming	Slope	*Ex*	*r*	$C_T \pm SEM^a$
ANF	dT_{VN}	−3.1	1.1	−1	14.66 ± 0.05
	Hexa	−2.0	2.2	−0.95	
	ANF_reverse	−3.1	1.1	−0.99	12.69 ± 0.07
GAPDH	dT_{VN}	−3.2	1.1	−1	16.25 ± 0.04
	Hexa	−3.1	1.1	−1	23.49 ± 0.03
	GAPDH_reverse	−3.3	1.0	−1	11.80 ± 0.06
HPRT	dT_{VN}	−3.2	1.1	−0.99	17.30 ± 10.10
	Hexa	−2.0	2.1	−0.88	
EF1α	dT_{VN}	−3.6	0.90	−1	14.95 ± 10.05
	Hexa	−2.2	1.9	−0.96	
MEF2C	dT_{VN}	−4.3	0.71	−1	18.99 ± 10.05
	Hexa	−3.7	0.87	−0.99	26.07 ± 10.13

Note. For abbreviations and explanation see Standard Curve under Materials and method.
[a] Calculated from six independent cDNA synthesis reactions using 1 μg of a single RNA sample.

found (*Ex* between 1.9 and 2.2). Finally, the most efficient cDNA priming methods were determined by comparing the average threshold cycles for six independent cDNA synthesis reactions per priming condition (Table 2, last column). For the PCR primer combinations tested, gene-specific priming was more efficient than oligo-dT_{VN} priming. This difference was PCR primer pair dependent and varied between 2 and 4.5 cycles for ANF and GAPDH, respectively. This is not entirely unexpected, as the spacing between the RT primer and PCR primer affects RT-PCR efficiency. For gene-specific priming there is no influence of spacing, whereas for oligo-dT_{VN} priming the distance between the reverse primer and the start of the poly-A-tail is 511 bp for GAPDH and 293 bp for ANF. Amplification curves obtained with hexamer priming were only reliable for GAPDH and MEF2C and were in these cases shifted seven cycles to the right compared to oligo-dT_{VN} priming. Therefore, hexamer priming could not be used or was far less sensitive than oligo-dT_{VN} priming.

In conclusion, gene-specific priming was most efficient, oligo-dT_{VN} priming was intermediately efficient, and hexamer priming was often unreliable. Although gene-specific priming is most efficient, it is less convenient compared to oligo-dT when relative expression levels of more than a single mRNA are measured. Gene-specific priming requires for each gene a separate cDNA reaction, whereas with oligo-dT a single reaction is sufficient.

Acknowledgments

We thank Marry Markman for technical support and Mr. C.J. Hersbach for help with the illustrations. This research is financially supported by the Netherlands Heart Foundation, Grants M96002 and 99.170.

References

[1] U.E.M. Gibson, C.A. Heid, P.M. Williams, A novel method for real time quantitative RT-PCR, Genome Methods 6 (1996) 951–1001.
[2] R. Rasmussen, in: S. Meuer, C. Wittwer, K. Nakagawara (Eds.), Rapid Cycle Real-Time PCR, Springer, Berlin, 2001, pp. 21–34.
[3] P. Kains, The PCR plateau phase—towards an understanding of its limitations, Biochim. Biophys. Acta 1494 (2000) 23–27.
[4] R.M. Clegg, Fluorescence resonance energy transfer and nucleic acids, Methods Enzymol. 211 (1992) 353–388.
[5] R. Selvin, Fluorescence resonance energy transfer, Methods Enzymol. 246 (1995) 300–334.
[6] V.A. Maltsev, J. Rohwedel, J. Hescheler, A.M. Wobus, Embryonic stem cells differentiate in vitro into cardiomyocytes representing sinusnodal, atrial and ventricular cell types, Mech. Dev. 44 (1993) 41–50.
[7] A.S. Kahn, A.S. Wilcox, J.A. Hopkins, J.M. Sikela, Efficient double stranded sequencing of cDNA clones containing long poly(A) tails using anchored poly(dT) primers, Nucleic Acids Res. 19 (1990) 1715.
[8] P. Liang, L. Averboukh, A.B. Pardee, Distribution and cloning of eukaryotic mRNAs by means of differential display: refinements and optimization, Nucleic Acids Res. 21 (1993) 3269–3275.
[9] K.M. Ririe, R.P. Rasmussen, C.T. Wittwer, Product differentiation by analysis of DNA melting curves during polymerase chain reaction, Anal. Biochem. 245 (1997) 154–160.
[10] A.C. Fijnvandraat, P.A.J. de Boer, R.H. Lekanne Deprez, A.F.M. Moorman, Non-radioactive in situ detection of mRNA in ES cell-derived cardiomyocytes ana the developing heart, Microsc. Res. Tech., in press.
[11] V.M. Christoffels, A.G.M. Kaiser, A.C. Houweling, D.E.W. Clout, A.F.M. Moorman, Patterning the embryonic heart: identification of five mouse Iroquois homeobox genes in the developing heart, Dev. Biol. 224 (2000) 263–274.